JOURNAL OF GEOPHYSICAL RESEARCH, VOL. 93, NO. A10, PAGES 11,445–11,454, OCTOBER 1, 1988

Mapping of Auroral Kilometric Radiation Sources to the Aurora

R. L. HUFF, W. CALVERT, J. D. CRAVEN, L. A. FRANK, AND D. A. GURNETT

Department of Physics and Astronomy, University of Iowa, Iowa City

Auroral kilometric radiation (AKR) and optical auroral emissions are observed simultaneously using plasma wave instrumentation and auroral imaging photometers carried on the DE 1 spacecraft. The DE 1 plasma wave instrument measures the relative phase of signals from orthogonal electric dipole antennas, and from these measurements, apparent source directions can be determined with a high degree of precision. Wave data are analyzed for several strong AKR events, and source directions are determined for several emission frequencies. By assuming that the AKR originates at cyclotron resonant altitudes, a candidate source field line is identified. When the selected source field line is traced down to auroral altitudes on the concurrent DE 1 auroral image, a striking correspondence between the AKR source field line and localized auroral features is produced. The magnetic mapping study provides strong evidence that AKR sources occur on field lines associated with discrete auroral arcs, and it provides confirmation that AKR is generated near the electron cyclotron frequency.

INTRODUCTION

The terrestrial magnetosphere is a source of intense electromagnetic radiation emitted at kilometric wavelengths. This very interesting emission is called auroral kilometric radiation (AKR) and has been studied by many investigators for more than a decade. *Dunckel et al.* [1970] first observed the low-frequency portion (< 100 kHz) of the AKR emission spectrum, then called high-pass noise, using the OGO 1 spacecraft, and reported that the kilometric radiation occurs primarily in the local nighttime region of the Earth. Later, *Gurnett* [1974], using the IMP 6 and IMP 8 satellites, found that AKR is most intense at frequencies between 50 and 500 kHz, originates from altitudes less than 3 Earth radii (R_E), in the auroral region, and occurs in sporadic bursts lasting up to several hours. The same study confirmed that AKR occurs in the local evening and presented evidence that the radiation is emitted in a wide cone with axis centered near 2200 hours MLT. Using images from the polar-orbiting DAPP reconnaissance satellite, *Gurnett* [1974] showed that AKR is closely correlated with the occurrence of structured auroral forms (discrete auroral arcs) in the evening auroral zone. Since discrete arcs were known to be directly associated with the energetic "inverted-V" electrons moving along auroral field lines [*Ackerson and Frank*, 1972], an association between inverted-V electron precipitation and AKR was inferred. This relationship was later confirmed by *Benson and Calvert* [1979] and *Benson et al.* [1980] using measurements from ISIS 1. Attempts were made by several groups to more accurately locate the AKR source region. Using data from Hawkeye 1 and IMP 8, *Kurth et al.* [1975] presented evidence that the average AKR source region is located between 1 and 2 R_E altitude at about 2200 hours MLT. These results were based on a direction-finding technique which involved analyzing the modulation in received electric field strength produced by the spacecraft rotation. *Kurth et al.* [1975] noted that considerable scatter was evident in the deduced source directions and suggested that this scatter was more likely due to actual variability in the location of the source with time than to statistical errors. Data from the lunar-orbiting RAE 2 were used by *Kaiser and Alexander* [1976] to produce two-dimensional AKR source location measurements. These investigators presented evidence confirming that the average source location for kilometric radiation (at 250 kHz) is above the polar regions at altitudes of 2–3 R_E. They also reported that some of the apparent sources seemed to be located at radial distances greater than 7 R_E, although these observations have since been attributed to scattering by density inhomogeneities [*Alexander et al.*, 1979]. *Alexander and Kaiser* [1976], again using lunar occultation data, reported that AKR emissions at higher frequencies originate nearer the Earth than emissions at lower frequencies. The authors also reported that nightside northern hemisphere sources are located along the 70° invariant latitude magnetic field line, which was later confirmed by *Benson and Calvert* [1979]. The propagation mode of AKR was investigated by *Gurnett and Green* [1978] using measurements from Hawkeye 1 and by *Benson and Calvert* [1979] and *Calvert* [1981] using data from ISIS 1. All of these studies concluded that AKR propagates in the right-hand polarized extraordinary mode and that, near the source, AKR is emitted nearly perpendicular to auroral field lines. Direct polarization measurements from the DE 1 plasma wave instrument [*Shawhan and Gurnett*, 1982; *Mellott et al.*, 1984; *Calvert*, 1985] confirmed that AKR propagates predominantly in a right-hand mode, although left-hand emissions sometimes also occur. *Benson and Akasofu* [1984] confirmed the correlation between AKR and the aurora by comparing ISIS 1 topside sounder data with visual auroral observations from the network of Alaskan all-sky camera stations. More recently, measurements from the Viking V4H experiment [*Bahnsen et al.*, 1987; *de Feraudy et al.*, 1987] have confirmed many of the propagation characteristics of AKR. Viking source region observations [*Bahnsen et al.*, 1987] also offer strong evidence that AKR is generated at the electron cyclotron frequency.

The purpose of the present study is to investigate the correspondence between AKR and the discrete aurora on time scales comparable to auroral substorms. A better understanding of the relationship between these two auroral processes should, in turn, provide insight into the mechanisms which control AKR and auroral processes in general. In this paper we present AKR direction-finding measurements derived from DE 1 plasma wave instrument data. The measurements are compared with concurrent optical auroral emissions as measured by the DE 1 auroral imagers.

Paper number 88JA03012.
0148-0227/88/88JA-03012$05.00

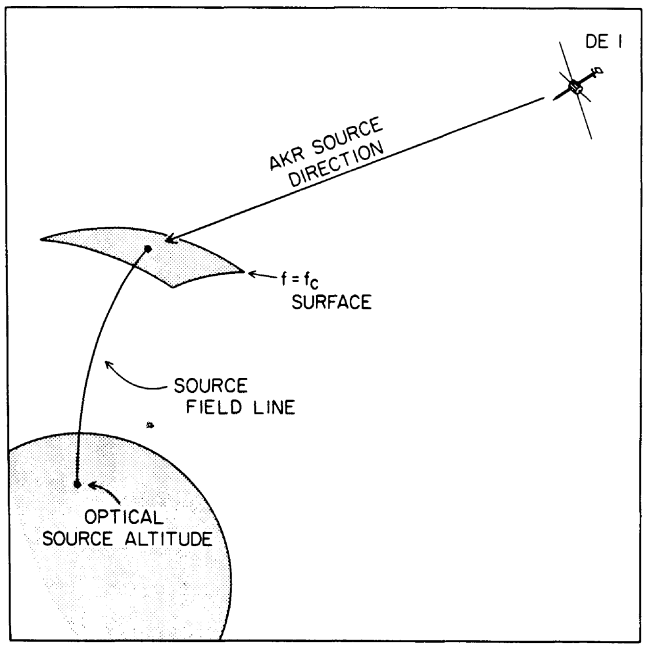

Fig. 1. Locating AKR sources using DE 1. The spacecraft is illuminated by an AKR source assumed to be located on the surface defined by $f = f_c$, where f_c is the electron cyclotron frequency. The AKR source position is determined by finding the intersection of the wave direction of arrival with the surface $f = f_c$. A magnetic field model is then used to map the source location to low altitudes for comparison with the aurora.

INSTRUMENTATION AND MEASUREMENT TECHNIQUE

The DE 1 spacecraft is the high-altitude member of a pair of spacecraft launched on August 3, 1981. DE 1 is in a polar orbit of 90° inclination with an apogee at 4.66 R_E geocentric radial distance and a perigee at an altitude of 675 km. The spacecraft carries an integrated set of instruments designed to provide measurements of global optical emissions, wave electric and magnetic fields, and charged particle intensities [*Hoffman et al.*, 1981]. This study makes use of data from the DE 1 plasma wave instrument (PWI) and the auroral imagers.

Global auroral imaging instrumentation carried on DE 1 provides images of the Earth's optical emissions at a variety of visible and vacuum ultraviolet (VUV) wavelengths. A description of this instrumentation is given by *Frank et al.* [1981]. The current study uses images with a 30° field of view which are obtained at VUV wavelengths.

The DE 1 plasma wave instrument provides measurements of electric and magnetic fields over a frequency range of 1 Hz to 2 MHz. A detailed description of the capabilities of the instrument is presented by *Shawhan et al.* [1981]. Here we will only provide a brief discussion of those elements of the wave instrument which are relevant to the current study, specifically, the step frequency correlator (SFC) and the E_x and E_z electric dipole antennas. The E_x electric antenna consists of a 200-m (tip to tip) dipole which lies in the spacecraft spin plane. The E_z antenna consists of a 9-m (tip to tip) dipole oriented along the spin axis. The SFC processes signals from two antennas and produces two 136-point logarithmically spaced spectrums covering the frequency range from 1.78 Hz to 410 kHz. The instrument completes a frequency sweep once every 32 s. In addition to amplitude information, the SFC also provides relative phase measurements between the two antenna signals at each frequency. This phase information may be interpreted in terms of wave polarization and provides a very accurate method for deducing wave directions [*Calvert*, 1985]. Assuming circular polarization, a point wave source located arbitrarily with respect to the spacecraft will produce a unique pattern of measured phase versus spacecraft spin angle, with a shape corresponding to a unique pair of source direction angles as defined by

$$\tan \phi = \pm \csc \beta \tan \alpha \qquad (1)$$

where ϕ is the measured relative phase, α is the angular position of the source relative to the nadir direction projected into the spacecraft spin plane, and β is the angle of the source out of the spin plane (equation (6) from *Calvert* [1985] contains a typographical error; "csc" is the correct function). The method has been used successfully to triangulate the AKR source position and confirm its approximate relationship to the local cyclotron frequency [*Calvert*, 1985] and to determine the source directions for harmonic AKR events [*Mellott et al.*, 1986].

Figure 1 illustrates the geometry of AKR direction finding with DE 1. For the purpose of this study, the AKR is assumed to originate at altitudes such that the wave frequency f is equal to the local electron cyclotron frequency f_c, as is suggested by the Viking observations [*Bahnsen et al.*, 1987]. By making this assumption it is possible (using the Magsat 2 magnetic field model) to find the intersection of the AKR source direction and the appropriate $f = f_c$ surface, as indicated in the figure, thus locating the source in three dimensions and at the same time identifying the magnetic field line from which the AKR originates.

Two other assumptions are implicit in this method for locating AKR sources. One cannot, by analyzing the phase response, differentiate between a circularly polarized wave which originates at some angle with respect to the spin plane, and a wave of nonzero ellipticity originating from a source more closely aligned with the spin plane [see *Calvert*, 1985, equation (5)]. For the purpose of analyzing the data for this study, AKR is assumed to be circularly polarized. The other assumption made for this study is that the curvature of AKR ray paths can be ignored. In other words, the ray path from the source to DE is assumed to be a straight line. Ray tracing studies, such as those described by *Calvert* [1981] and *Hashimoto* [1984], indicate that a straight-line approximation is acceptable given the range of reception geometries encountered by DE 1 for observations used in this study.

Data selection for the present investigation was accomplished in the following manner. For the first six months of DE operations, all of the intervals during which the PWI was in the proper E_x/E_z antenna mode were identified. Since the PWI has many operational modes, only about 100 such cases were found. Two-hour frequency-time spectrograms were then examined for AKR signatures, and those intervals showing no AKR or weak AKR were excluded from the data set. The exclusion of weak AKR cases was necessary since the relatively low sensitivity E_z antenna sets a lower limit to the signal strength below which phase measurements could not be obtained. About 50 of the intervals were excluded from the study on this basis. Next, the remaining intervals were examined for the variability of simultaneous global images. As coverage during this period was extensive, only a few AKR intervals were excluded for lack of images. Finally, the remaining cases were sorted according to the visual complexity of the aurora.

Since the PWI responds to superposed signals, it was felt that a compact and spatially simple AKR source would be the easiest to characterize, and that a source of this type would most likely correspond to a single bright feature in the aurora or to a geometrically simple arc structure. Of the original 100 intervals, 14 were found to have this type of aurora. These cases were analyzed in detail, and the data and results from four of these intervals are presented in this paper.

The direction-finding analysis was performed by segmenting the data into frequency-time blocks of about 50 kHz by 5 min. Although a direction of arrival can be derived during a single 6-s spin of the spacecraft, 5-min intervals provide better accuracy, since more data points are available for the least squares fit to the source direction function (equation (1)). The 5-min AKR segments were checked for high cumulative correlation in the phase measurement, and the direction angles with a satisfactory least squares fit were plotted on the concurrent auroral image as an apparent AKR source direction. The source was then located in three dimensions by finding the intersection of the line-of-sight ray path with the $f = f_c$ surface. As a final step, the magnetic field model was used to trace the source field line down into the ionosphere to an assumed optical source altitude of 200 km (see Figure 1).

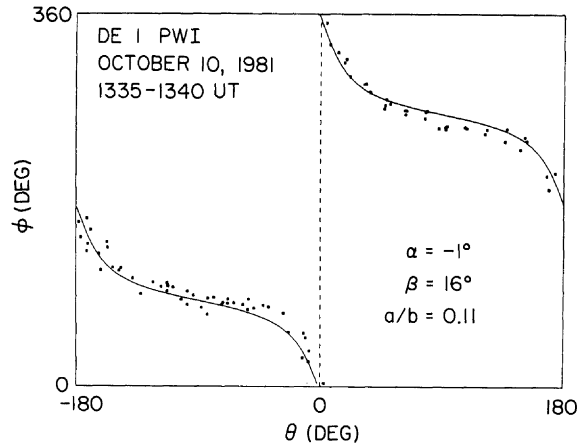

Fig. 2. Measured phase (ordinate) versus spacecraft rotation (abscissa). The figure shows data points accumulated over the interval 1335–1340 UT and the result of the least squares fit to equation (1). Derived source direction angles α and β are indicated in the panel.

OBSERVATIONS

Plate 1 presents an example of a strong kilometric radiation event observed by DE 1 on October 10, 1981. The format of the PWI data is a 2-hour spectrogram containing the full frequency range of the SFC. The left uppermost panel shows the electric field spectral density as a function of time and frequency, and the bottom left panel shows the wave polarization, where red represents right-hand polarization with respect to the zenith and green represents left-hand polarization. In both panels the white line labeled f_{ce} is the local electron cyclotron frequency. The relevant auroral image obtained at vacuum ultraviolet wavelengths (123–155 nm) is shown to the right.

During this time interval the frequency range above the electron cyclotron frequency is dominated by AKR emissions which extend from the beginning of the plot at 1300 UT, until about 1425 UT, with the strongest AKR occurring at about 1355 UT. For frequencies below f_{ce}, between 1320 UT and 1400 UT, auroral hiss can be seen extending up to the electron plasma frequency f_{pe}, and strong electrostatic bursts are observed between 1350 UT and 1410 UT at frequencies below 10 kHz. The brief change in intensity which extends over the entire frequency range of the instrument, and which occurs at 1353 UT, is due to a change in instrument mode. Source direction angles for this AKR event are deduced by performing a least squares fit to the phase data beginning at 1335 UT, and at frequencies centered at 170, 218, and 281 kHz. An example of the phase versus spacecraft rotation plot showing the measured data points for a narrow range of frequencies centered on 218 kHz is shown in Figure 2. A solid line superimposed on the data indicates the least squares fit. The auroral image in Plate 1 shows the spacecraft view of the Earth from about 60° northern magnetic latitude in the midevening sector. Antisunward of the terminator, a conspicuous brightening of the auroral oval is observed near late evening with maximum brightness along the poleward edge. AKR source directions as observed from the spacecraft are superposed on the image with the numbers 1, 2, and 3 corresponding to frequencies of 170, 218, and 281 kHz, respectively. Magnetic field lines selected by assuming that AKR is produced at the electron cyclotron frequency surface are shown as dashed lines. This example illustrates an excellent correspondence between the measured AKR sources and the aurora, since the magnetic field line through the AKR source for each frequency clearly passes through the brightest auroral region.

Another example of AKR observed with the DE 1 wave instrument is presented in Plate 2. These observations from 0320 to 0520 UT on January 27, 1982, are presented here because they illustrate another interesting aspect of the AKR source location results. Source directions are deduced for the 5-min interval commencing at 0445 UT. This specific time was chosen because the AKR is relatively broad in frequency, thereby offering the opportunity to locate AKR sources at different frequencies in order to verify that the source altitude changes with wave frequency. When the direction angles are plotted on the image shown in Plate 2, the expected frequency-altitude dependence is clearly demonstrated. AKR source directions for frequencies of 104, 136, 170, and 218 kHz are superposed on the image and are identified by the numbers 1–4, respectively. The viewing position, which was from about 55° northern magnetic latitude in the early morning sector, shows an ordered distribution of sources over a range of altitudes with lowest-frequency sources corresponding to highest altitude. Although the morphology of the aurora in this example is somewhat different from that of the previous case, the selected source field lines clearly converge to the brightest feature along the auroral oval.

The third AKR interval selected for this study is from observations in the time interval 2020–2144 UT on September 28, 1981, and is illustrated in Plate 3. The electric field spectrogram shows intense AKR over nearly the entire interval, as the spacecraft moves through decreasing altitudes toward the plasmapause. Source direction angles are derived from a 5-min segment of data beginning at 2109 UT for frequencies of 136, 170, 218, and 281 kHz. The simultaneous image at VUV wavelengths shows the spacecraft view of the aurora from about 55° northern magnetic latitude in the late evening sector. The altitude of DE 1 for this case is slightly lower than for the two previous examples. As before, the numbers 1–4 denote AKR source locations at the four frequencies. The au-

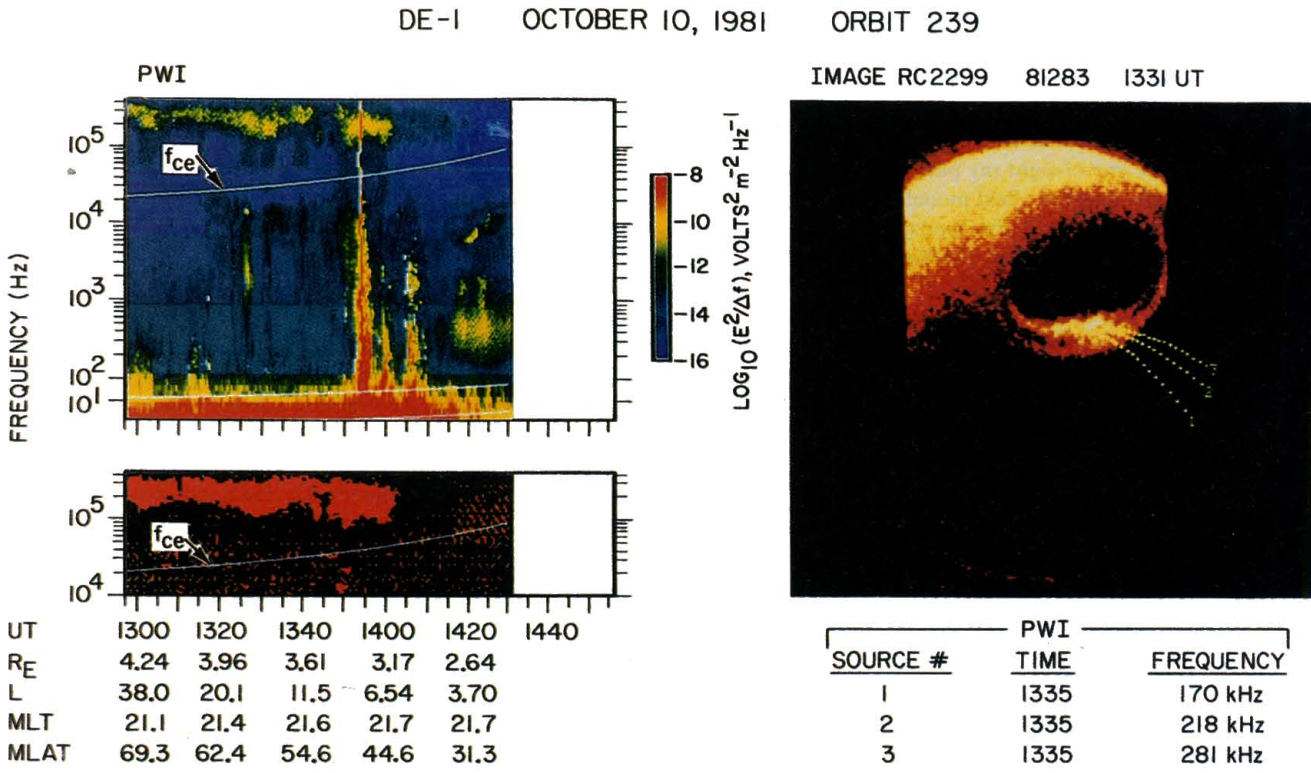

Plate 1. Electric field and polarization spectrograms and auroral image from October 10, 1981. The VUV image spans 12 min beginning at 1331 UT. AKR source positions were derived for three different frequencies using wave data from the time interval 1335–1440 UT. These positions are indicated on the concurrent auroral image by the points labeled 1, 2, and 3. Dashed lines show magnetic field lines traced downward from the associated AKR source positions. The source field lines are seen to converge on the brightest region of the aurora.

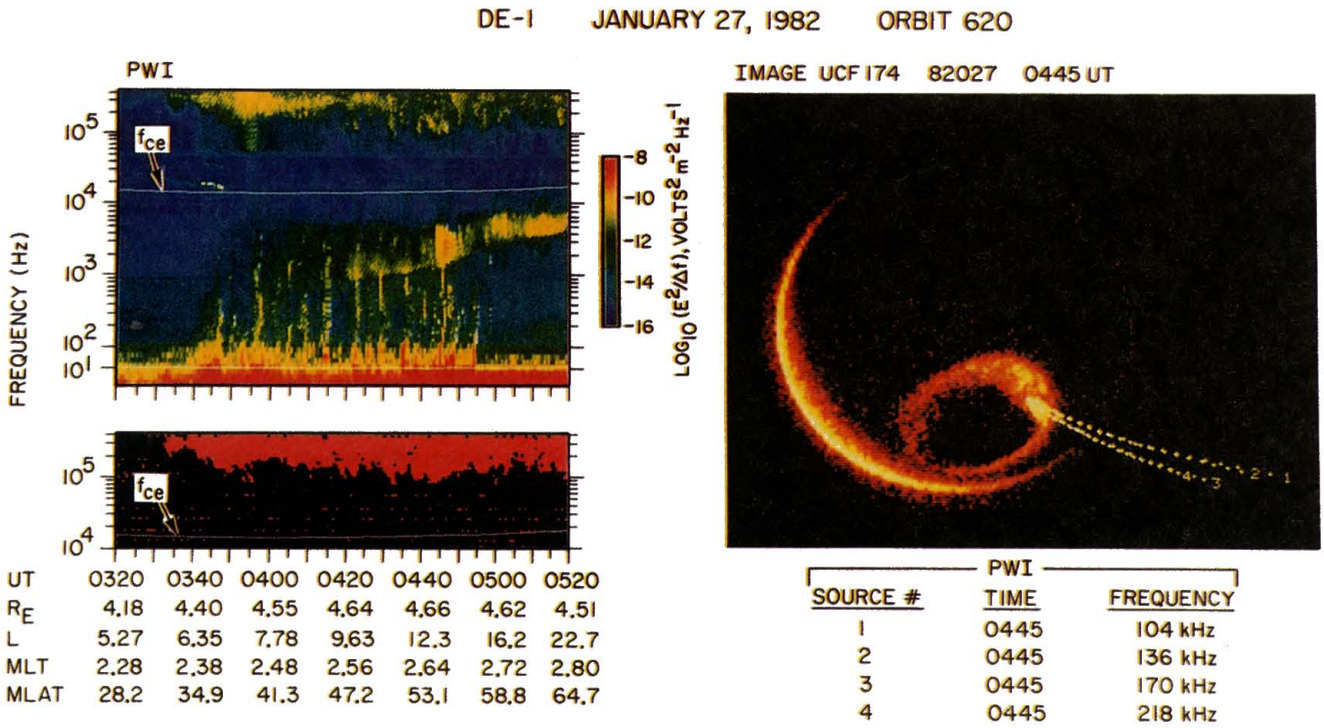

Plate 2. Electric field and polarization spectrograms and auroral image from January 27, 1982. Source directions were derived for the 5-min interval beginning at 0445 UT and for a selection of frequencies indicated at the bottom of the auroral image. The deduced AKR source positions (shown by numbered points on the image) map accurately to the brightest region of the auroral oval and also show the expected increase in source altitude with decreasing wave frequency.

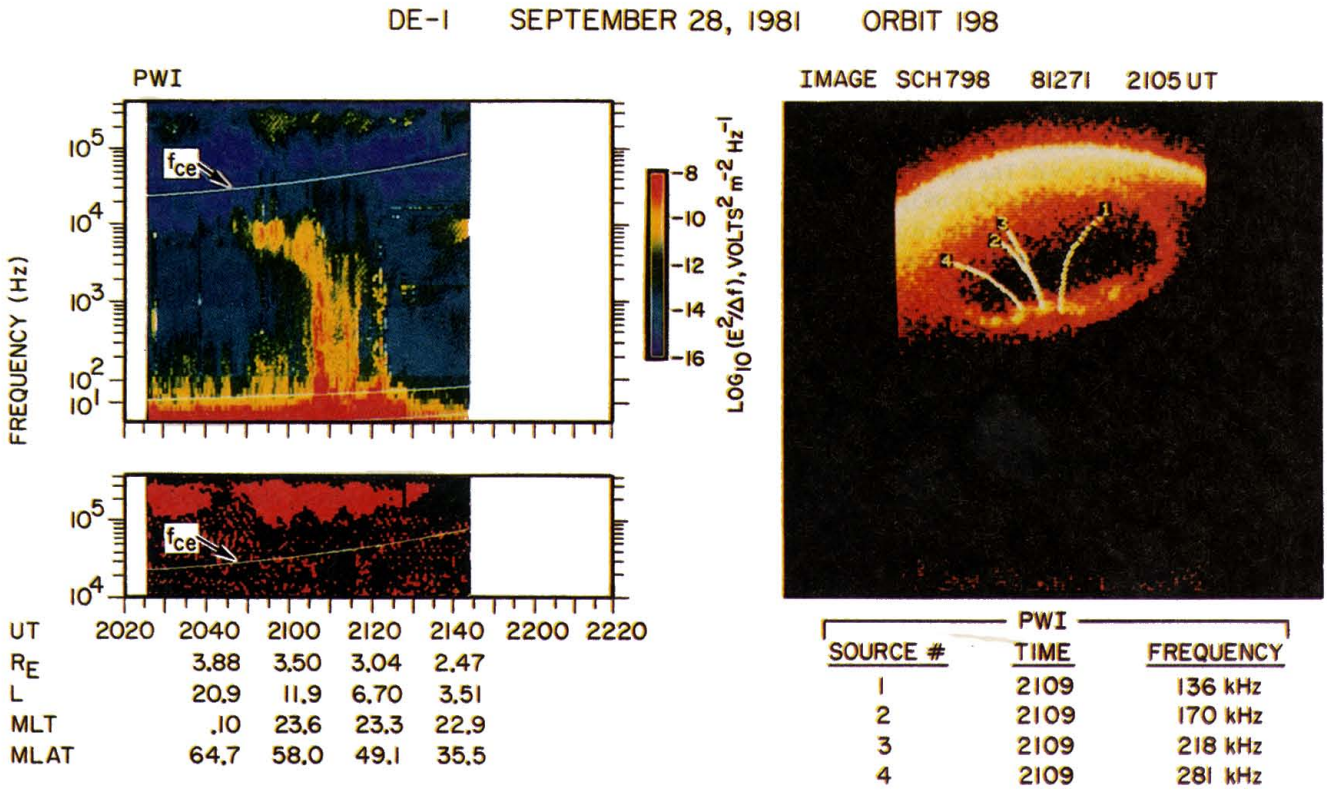

Plate 3. Observations similar to Plates 1 and 2 for an AKR event from September 28, 1981. Source directions were derived for the interval 2109–2113 UT for the frequencies indicated. The AKR source locations show a broad longitudinal distribution and map systematically to bright regions along the auroral oval.

roral image identifies a longitudinally extended discrete auroral form with several localized areas of enhanced luminosities. Candidate source field lines for this example, when plotted on the image, appear to map to different bright regions along the auroral oval, and the indicated longitudinal distribution of bright auroral emissions and associated AKR sources falls within the angular size of the statistical AKR source region as defined by earlier efforts [*Benson and Calvert*, 1979, Figure 5]. It should be noted that in this example, AKR sources are identified for different emission frequencies. Since the PWI responds to the dominant signal at a given frequency, regardless of the location of the source, this example also supports the concept of many widely spaced AKR sources operating simultaneously, although the sources are radiating at different power levels for different frequencies.

The final example presented here (Plate 4) is from January 4, 1982, and provides a striking illustration of the correspondence between AKR sources and the discrete aurora during what appears to be a weak substorm. DE 1 is positioned near apogee in the northern hemisphere, moving toward higher latitudes in the morning sector. Auroral images obtained throughout the period 0655–1135 UT at visible and VUV wavelengths identify the presence of nearly continuous, low-level auroral activity. In the electric field spectrogram, AKR can be seen above 100 kHz during the entire 2-hour interval, 0820–1020 UT. Source direction angles are derived for the time period from 0900 UT through 1000 UT, for a narrow range of frequencies centered at 218 kHz. The derived source locations and source field lines are shown overlaid on a sequence of six images presented at the bottom of Plate 4 (Plates 4*a*–4*f*). The first image of the sequence (0857–0909 UT) shows that the AKR source maps accurately to the brightest part of a discrete auroral form located along the poleward edge of the evening auroral oval. The next image (0909–0921 UT), seen in Plate 4*b*, shows the same precise correspondence between AKR source and optical structure, with the bright region of the discrete aurora located farther to the east and slightly poleward of the diffuse oval. The following two images (Plate 4*c* at 0921–0933 UT and Plate 4*d* at 0933–0946 UT) show that the discrete aurora is moving poleward. Although the aurora is now characterized by a system of bright regions, the selected source field line still maps to a point roughly centered on the bright areas. The final two 12-min images in the sequence are presented in Plates 4*e* and 4*f*. The discrete aurora is now more uniformly bright over its entire length and has moved poleward to the extent that it is now widely separated from the diffuse aurora at lower latitudes. Although the AKR source locations do not always map to the brightest features in the discrete aurora, they can be seen to map accurately and preferentially to the arc system, as opposed to any other distinct region of the aurora. It should be noted that the poleward motions of the discrete aurora in this small substorm are consistent with the motions analyzed for other pulsations [e.g., *Craven and Frank*, 1985, 1987].

MEASUREMENT ERRORS

An indication of the sensitivity of the mapping to uncertainties in the analysis is provided by Plates 5 and 6. These figures show the first image of the sequence of images from January 4, 1982 (see Plate 4).

Uncertainty in the relative phase measurements, whether due to sampling errors, imprecise attitude information, calibration bias, or errors in the least squares fit, translates directly into uncertainty in the deduced source direction angles α (angle in the spacecraft spin plane) and β (angle out of the spacecraft spin plane). In Plate 5, case 1 represents the AKR source direction at 218 kHz, and the associated source field line very accurately maps to the brightest part of the discrete aurora. The sources labeled 2 and 3, however, represent direction angles which have been arbitrarily adjusted by 2° in order to illustrate the effect of a small error in source direction on the mapping to the aurora. Sources 1, 2, and 3 therefore correspond to the source directions (α, β), $(\alpha + 2°, \beta + 2°)$, and $(\alpha - 2°, \beta - 2°)$, respectively. The source field lines associated with points 2 and 3 can be seen to map to regions which are clearly outside the auroral oval, indicating that a deviation of 2°, although a relatively small angle, represents a significant error within the context of the mapping study.

Another potential source for error in the mapping lies in the determination of the AKR source location along the line-of-sight ray path. As was discussed earlier, this location is determined by identifying the altitude along the ray path at which the local electron cyclotron frequency equals the frequency of the observed AKR. Since phase data are collected in frequency bins of about 50 kHz, the frequency of the dominant AKR component is known with a certainty of only ± 25 kHz, or for a frequency bin centered at 200 kHz, within about 10%.

Plate 6 illustrates the effect of such uncertainties on the magnetic mapping. It shows two hypothetical sources (labeled 1 and 2) along the same line of sight as that measured for 218 kHz in Plate 4*a* but interpreting the altitudes for cyclotron resonance at 170 and 281 kHz instead. In both cases, the mapped field lines clearly miss the bright aurora. This implies that such errors in choosing the intercept altitude, equivalent to frequency deviations of about 25%, would have been detectable.

The good fit of the mapped field line in this case, labeled 1 in Plate 4*a* and in Plate 5, thus confirms the roughly 1% precision of the technique previously estimated from the quality of the least squares fits [*Calvert*, 1985]. It also confirms that the AKR originates from near the electron cyclotron frequency with a frequency uncertainty of not more than 25%.

DISCUSSION

The four cases presented here are representative of the 14 cases analyzed. In all cases where the measured correlations are high and the aurora is reasonably well localized, excellent fits are obtained between the mapped source field lines and bright features of the aurora. When the aurora is dominated by a single bright feature, as it is in Plate 2, the source field lines invariably pass through that feature. For time scales of 10 min or less, this correspondence clearly confirms that to a high degree of precision the observed AKR originates from cyclotron resonant altitudes on auroral field lines.

Directional measurement errors of roughly 1° at about 3 R_E distance imply spatial localization of the source with respect to the field line within about 300 km, or equivalently, frequency localization with respect to the cyclotron frequency of about 10%. In a previous study [*Calvert*, 1985] involving triangulation to the AKR source region from different points along the DE 1 orbit (without the aid of auroral images), the corresponding precision was about 0.3 R_E (2000 km) and 35%, the difference being attributed primarily to changes of the aurora during the 2-hour interval between observations. The new measurements, moreover, although made at the much higher altitudes encountered by DE 1, yield localizations of

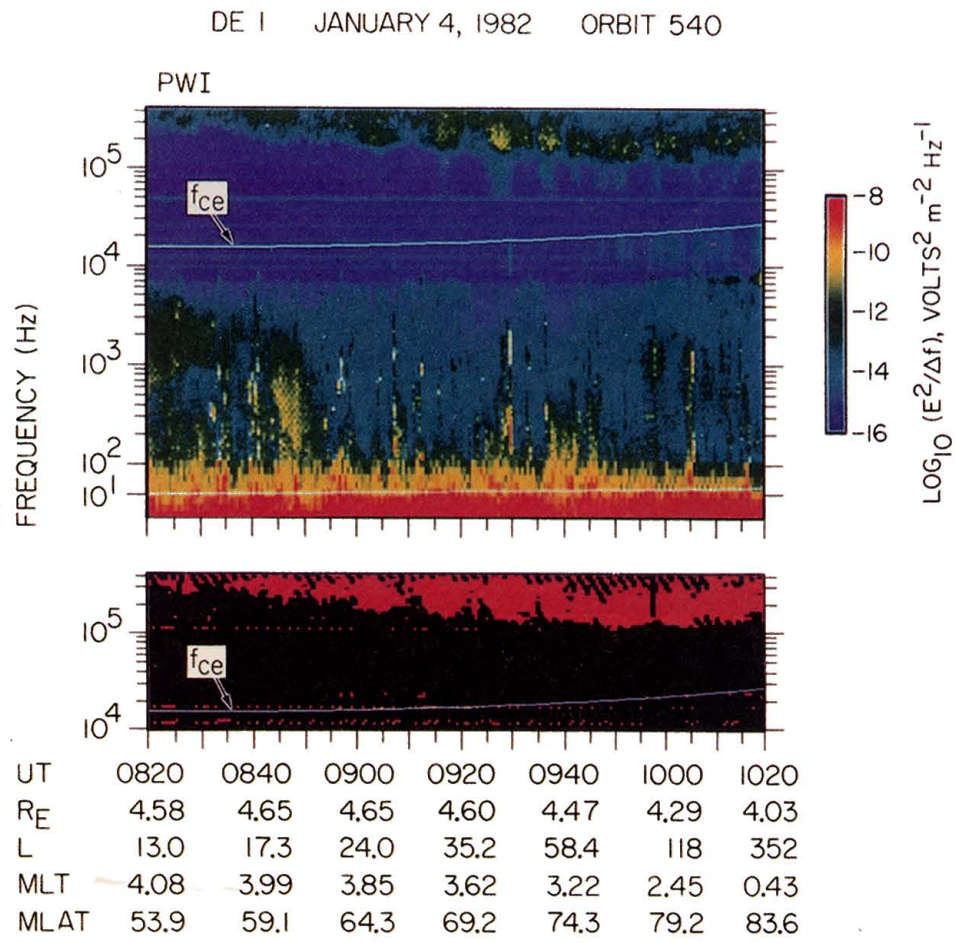

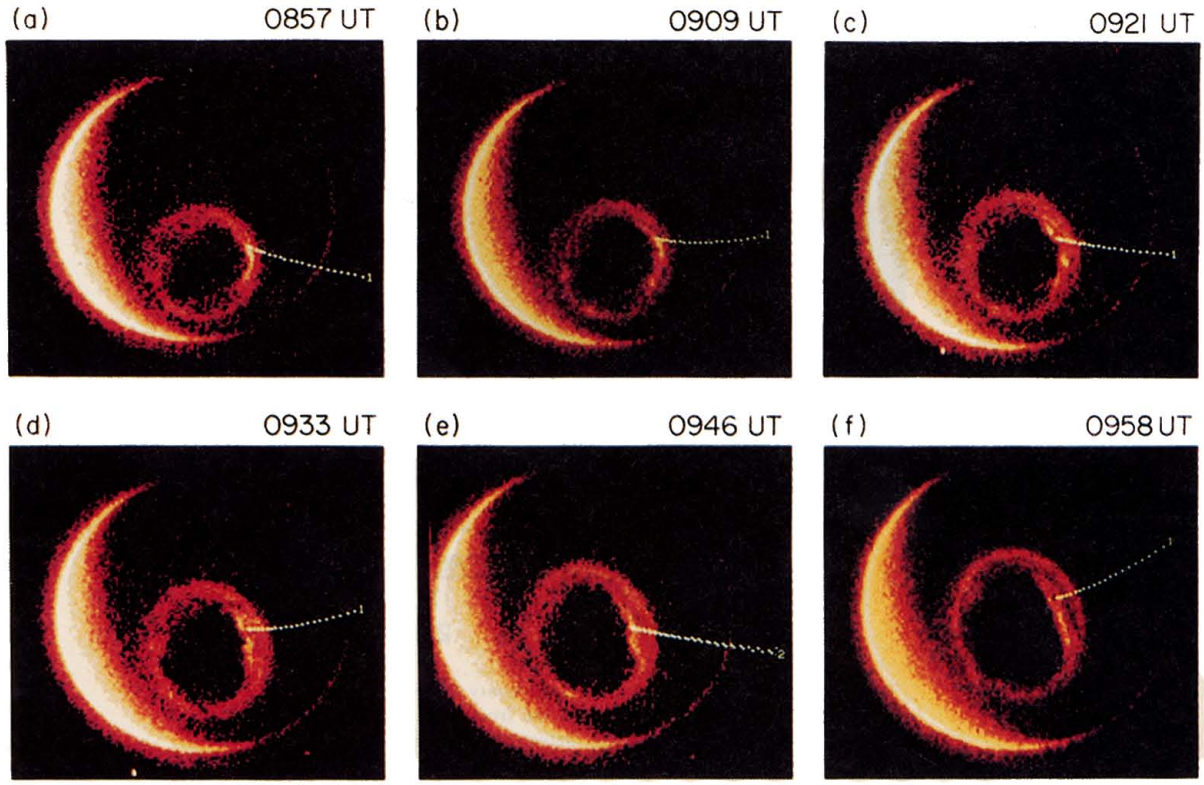

Plate 4. Electric field and polarization spectrograms and a sequence of six auroral images from January 4, 1982. The sequence of images shown in Plates 4*a*–4*f* covers about an hour and reveals what appears to be a weak substorm. AKR source locations derived from PWI data map preferentially to the discrete aurora even when the arc system has moved poleward of the diffuse aurora.

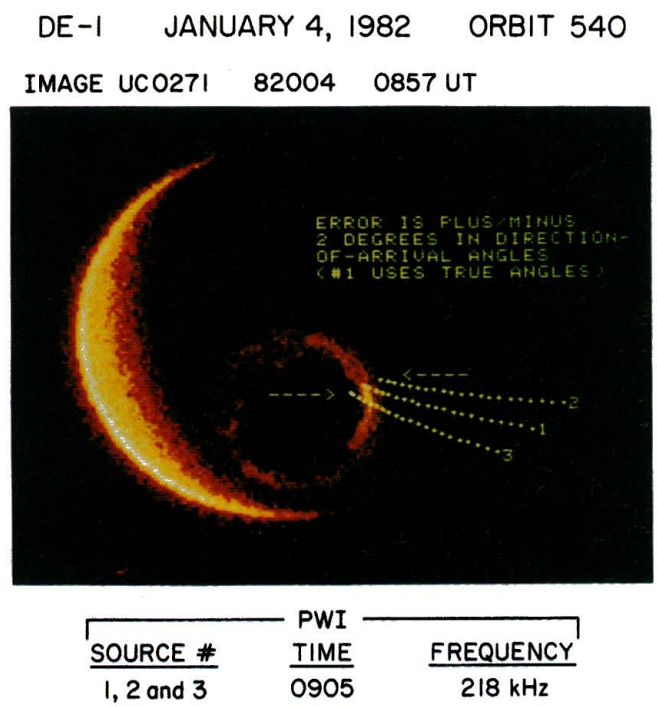

Plate 5. Image from January 4, 1982 (same as Plate 4*a*). An error of 2° in derived source direction angles causes a significant error in the mapping between AKR source and auroral features. The distorted source locations (labeled 2 and 3) map to regions outside the auroral oval.

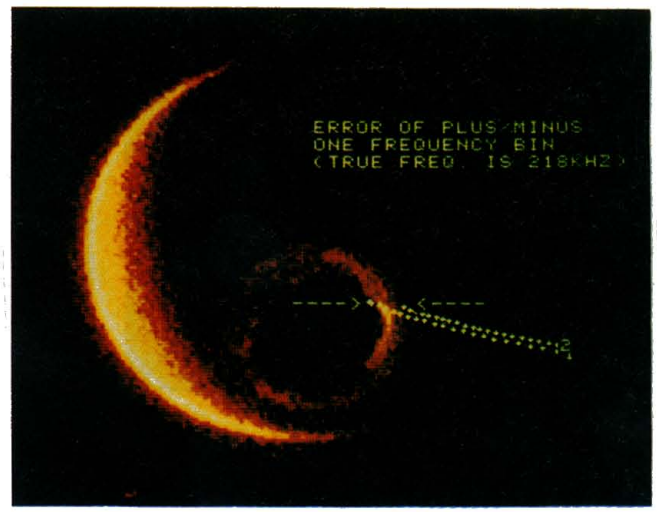

Plate 6. Same image as Plate 5. Uncertainty in selecting the correct intercept altitude, equivalent to one frequency bin, results in detectable errors in the mapping between AKR source and the aurora.

AKR sources with respect to the electron cyclotron frequency which are nearly as precise as those deduced from direct encounters with AKR sources by ISIS 1 [*Calvert*, 1981] and Viking [*Bahnsen et al.*, 1987]. The DE results complement the findings of *Benson and Akasofu* [1984], who reported a high degree of correlation between intense AKR and bright aurora. The global scale of the DE measurements provides additional perspective, since the results reported by *Benson and Akasofu* [1984] were based on low-altitude AKR source region encounters and field line mappings to aurora observed from the ground.

The direct association between AKR and the aurora, originally deduced by *Gurnett* [1974] from occurrence patterns seen over time scales of an hour, is clearly confirmed by these new observations. Additionally, these new measurements show that AKR sources and the discrete aurora are located on common auroral field lines and that when arcs move in latitude, as shown in the sequence in Plates 4*a*–4*f*, the AKR source appears to follow that motion. The persistence of the association in the context of the dynamic aurora demonstrates clearly that the AKR and the aurora are closely related, i.e., the AKR source position may be coincident with the low-altitude acceleration region for the precipitating energetic electrons that produce the luminosities, or at least it occupies the same field line as the acceleration region.

The sequence in Plate 4 also demonstrates that during a substorm the strongest AKR is generally associated with the most intense arcs at the poleward edge of the auroral oval. Because the DE 1 correlator must average over all of the radiation that it receives, the radiation from such locations can dominate over the radiation emitted from all other regions of the aurora. The apparent area ratios of auroral features as seen in the images suggest that the power of the locally produced AKR is 1 or 2 orders of magnitude stronger than that produced elsewhere.

The confirmation of the AKR source altitude, in which the cyclotron resonant source location can be directly visualized, should remove much of the uncertainty which remains regarding the origin of AKR at the electron cyclotron frequency. The analysis presented here is completely independent of previous studies which produced similar conclusions [*Gurnett*, 1974; *Gurnett and Green*, 1978; *Benson and Calvert*, 1979; *Calvert*, 1981], and the results are of sufficient precision as to strongly support AKR theories which require cyclotron resonance.

The accurate mappings also tend to confirm the assumption of circular polarization which, if assumed erroneously, would produce systematic errors in the mappings. Approximately circular polarization is verified by two separate aspects of the analysis. First, it is indicated in the least squares fit of the phase function in Figure 2 by the relatively low value for the parameter a/b, which is related to the ratio of the principal axes of the polarization ellipse [see *Calvert*, 1985, equation (5)]. Although not a completely unambiguous indicator owing to the unknown orientation of the polarization ellipse with respect to the DE 1 spin plane, the fitted value for a/b of 0.11 would imply a polarization ellipse axis ratio of about 1.1 to 1. Second, in determining the apparent ray direction we have explicitly assumed that β could be approximated by β/b, i.e., that the value of b is near that of unity for circular polarization. Since this works well for angles as large as 20°, within a precision of about 1°, the implication is that b is within only a few percent of unity, suggesting circularly polarized waves.

The accurate mappings also tend to support the assumption of straight-line ray paths, suggesting that the electron density along the ray paths must be quite low ($f_p \ll f$). The lack of measurable bias due to curved ray paths also suggests that there is little need for the use of ray tracing techniques in analyzing the examples presented here. On the other hand, ray tracing should still be important for the complete determination of ray paths which encounter the higher plasma densities of the plasmasphere or polar cap. Also, if AKR is always emitted at large angles with respect to the source mangnetic field, wave refraction very near the source would still seem to be the most likely explanation.

CONCLUSIONS

In this study, AKR source locations are identified with particular magnetic field lines and mapped down to the aurora. Within an angular precision of about 1°, corresponding to a spatial precision of about 300 km and a frequency precision of about 10%, it is found that the dominant, extraordinary mode component of the AKR invariably originates from cyclotron resonant altitudes on field lines which map to bright auroral features. This clearly confirms the close association between AKR and the discrete aurora [*Gurnett*, 1974] and supports theories which require generation of the AKR at the electron cyclotron frequency.

These results strongly suggest that the AKR is generated by the Doppler-shifted cyclotron resonance instability of *Melrose* [1976] and *Wu and Lee* [1979], since no other known mechanism can produce emissions at frequencies so close to the electron cyclotron frequency. A comprehensive model of the AKR generation, however, must also explain the observed spectral fine structure [*Gurnett et al.*, 1979] by means of radio wave lasing [*Calvert*, 1982] or some other mechanism and must, at the same time, accommodate the recent observations of ordinary mode and harmonic components [*Mellott et al.*, 1984, 1986].

Acknowledgments. The authors wish to thank M. R. Dvorsky, T. L. Barnett-Fisher, and J. E. Chrisinger for their uniformly excellent efforts in software preparation, assistance in data processing, and graphics support, respectively. This research has been supported through grants NAG5-310 and NAG5-483 with Goddard Space Flight Center, grants NGL 16-001-043 and NGL 16-001-002 with NASA Headquarters, and contract N00014-85-K-0404 with the Office of Naval Research.

The Editor thanks A. Bahnsen and R. F. Benson for their assistance in evaluating this paper.

REFERENCES

Ackerson, K. L., and L. A. Frank, Correlated satellite measurement of low-energy electron precipitation and ground-based observations of a visible auroral arc, *J. Geophys. Res.*, *77*, 1128, 1972.

Alexander, J. K., and M. L. Kaiser, Terrestrial kilometric radiation, 1, Spatial structure studies, *J. Geophys. Res.*, *81*, 5948, 1976.

Alexander, J. K., M. L. Kaiser, and P. Rodriguez, Scattering of terrestrial kilometric radiation at very high altitudes, *J. Geophys. Res.*, *84*, 2619, 1979.

Bahnsen, A., J. Mogens, E. Ungstrup, and I. B. Iversen, Auroral hiss and kilometric radiation measured from the Viking satellite, *Geophys. Res. Lett.*, *14*, 471, 1987.

Benson, R. F., and S.-I. Akasofu, Auroral kilometric radiation/aurora correlation, *Radio Sci.*, *19*, 527, 1984.

Benson, R. F., and W. Calvert, ISIS 1 observations at the source of auroral kilometric radiation, *Geophys. Res. Lett.*, *6*, 479, 1979.

Benson, R. F., W. Calvert, and D. M. Klumpar, Simultaneous wave and particle observations in the auroral kilometric radiation source region, *Geophys. Res. Lett.*, *7*, 959, 1980.

Calvert, W., The signature of auroral kilometric radiation on ISIS 1 ionograms, *J. Geophys. Res.*, *86*, 76, 1981.

Calvert, W., A feedback model for the source of auroral kilometric radiation, *J. Geophys. Res.*, *87*, 8199, 1982.

Calvert, W., DE 1 measurements of AKR wave directions, *Geophys. Res. Lett.*, *12*, 381, 1985.

Craven, J. D., and L. A. Frank, The temporal evolution of a small substorm as viewed from high altitudes with Dynamics Explorer 1, *Geophys. Res. Lett.*, *12*, 465, 1985.

Craven, J. D., and L. A. Frank, Latitudinal motions of the aurora during substorms, *J. Geophys. Res.*, *92*, 4565, 1987.

de Feraudy, H., B. M. Pedersen, A. Bahnsen, and M. Jespersen, Viking observations of auroral kilometric radiation from the plasmasphere to night auroral oval source regions, *Geophys. Res. Lett.*, *14*, 511, 1987.

Dunckel, N., B. Ficklin, L. Rorden, and R. A. Helliwell, Low-frequency noise observed in the distant magnetosphere with OGO 1, *J. Geophys. Res.*, *75*, 1854, 1970.

Frank, L. A., J. D. Craven, K. L. Ackerson, M. R. English, R. H. Eather, and R. L. Carovillano, Global auroral imaging instrumentation for the Dynamics Explorer Mission, *Space Sci. Instrum.*, *5*, 369, 1981.

Gurnett, D. A., The Earth as a radio source: Terrestrial kilometric radiation, *J. Geophys. Res.*, *79*, 4227, 1974.

Gurnett, D. A., and J. L. Green, On the polarization and origin of auroral kilometric radiation, *J. Geophys. Res.*, *83*, 689, 1978.

Gurnett, D. A., R. R. Anderson, F. L. Scarf, R. W. Fredricks, and E. J. Smith, Initial results from the ISEE-1 and -2 plasma wave investigation, *Space Sci. Rev.*, *23*, 103, 1979.

Hashimoto, K., A reconciliation of propagation modes of auroral kilometric radiation, *J. Geophys. Res.*, *89*, 7459, 1984.

Hoffman, R. A., G. D. Hogan, and R. Maehl, Dynamics Explorer spacecraft and ground operations systems, *Space Sci. Instrum.*, *5*, 349, 1981.

Kaiser, M. L., and J. K. Alexander, Source location measurement of terrestrial kilometric radiation obtained from lunar orbit, *Geophys. Res. Lett.*, *3*, 37, 1976.

Kurth, W. S., M. M. Baumback, and D. A. Gurnett, Direction-finding measurements of auroral kilometric radiation, *J. Geophys. Res.*, *80*, 2764, 1975.

Mellott, M. M., W. Calvert, R. L. Huff, D. A. Gurnett, and S. D. Shawhan, DE-1 observations of auroral kilometric radiation in the ordinary and extraordinary wave modes, *Geophys. Res. Lett.*, *11*, 1188, 1984.

Mellott, M. M., R. L. Huff, and D. A. Gurnett, DE 1 observations of harmonic auroral kilometric radiation, *J. Geophys. Res.*, *91*, 13,732, 1986.

Melrose, D. B., An interpretation of Jupiter's decametric radiation and the terrestrial kilometric radiation as direct amplified gyroemission, *Astrophys. J.*, *207*, 651, 1976.

Shawhan, S. D., and D. A. Gurnett, Polarization measurements of auroral kilometric radiation by Dynamics Explorer-1, *Geophys. Res. Lett.*, *9*, 913, 1982.

Shawhan, S. D., D. A. Gurnett, D. L. Odem, R. A. Helliwell, and C. G. Park, The plasma wave and quasi-static electric field instrument (PWI) for Dynamics Explorer A, *Space Sci. Instrum.*, *5*, 535, 1981.

Wu, C. S., and L. C. Lee, A theory of the terrestrial kilometric radiation, *Astrophys. J.*, *230*, 621, 1979.

W. Calvert, J. D. Craven, L. A. Frank, D. A. Gurnett, and R. L. Huff, Department of Physics and Astronomy, University of Iowa, IA 52242.

(Received August 14, 1987;
revised May 23, 1988;
accepted June 9, 1988.)